Complex antiferromagnetic order in $Dy_3Ag_4Sn_4$

2006 J. Phys.: Condens. Matter 18 5783

(http://iopscience.iop.org/0953-8984/18/24/018)

INSTITUTE OF PHYSICS PUBLISHING JOURNAL OF PHYSICS: CONDENSED MATTER

J. Phys.: Condens. Matter **18** (2006) 5783–5792 doi:10.1088/0953-8984/18/24/018

Complex antiferromagnetic order in $Dy_3Ag_4Sn_4$

Laura K Perry[1], J M Cadogan[2], D H Ryan[1,5], F Canepa[3], M Napoletano[3], D Mazzone[4] and P Riani[4]

[1] Department of Physics, McGill University, Montreal, H3A 2T8, Canada
[2] School of Physics, The University of New South Wales, Sydney NSW 2052, Australia
[3] Dipartimento di Chimica e Chimica Industriale, Via Dodecaneso 31, 16146 Genova, Italy
[4] INSTM and Dipartimento di Chimica e Chimica Industriale, Via Dodecaneso 31, 16146 Genova, Italy

E-mail: dhryan@physics.mcgill.ca

Received 10 March 2006
Published 2 June 2006
Online at stacks.iop.org/JPhysCM/18/5783

Abstract

We have studied the complex magnetic ordering of the Dy sublattices in orthorhombic $Dy_3Ag_4Sn_4$ by high-resolution neutron diffraction and ^{119}Sn Mössbauer spectroscopy. Magnetic ordering in this compound occurs over two transitions. At 16 K the Dy(2d) site orders in a doubled commensurate antiferromagnetic structure described by a propagation vector [0 $\frac{1}{2}$ 0], with moments aligned along [100]. The Dy(4e) site orders incommensurately with a propagation vector [0 0.628(1) 0] and moments in the (001) plane. Below the second transition at 14 K both Dy site ordering modes are commensurate antiferromagnetic with the propagation vector [0 $\frac{1}{2}$ 0] and unchanged ordering directions. The ^{119}Sn Mössbauer spectra comprise three magnetically split sextets in the area ratio 50%:25%:25% due to transferred hyperfine fields at the ^{119}Sn nuclei from the surrounding magnetic Dy neighbours. This spectral decomposition deviates from the area ratio 50%:50% expected on the basis of the crystal structure and is in perfect agreement with the magnetic structure of $Dy_3Ag_4Sn_4$ deduced from neutron diffraction data.

(Some figures in this article are in colour only in the electronic version)

1. Introduction

The $R_3T_4X_4$ compounds (R = rare-earth; T = Cu, Ag, Pd; X = Si, Ge and Sn) form in the orthorhombic $Gd_3Cu_4Ge_4$ structure [1] with the *Immm* (#71) space group. It is now well established that the magnetic ordering of these compounds is antiferromagnetic and involves only the R atoms, which occupy the 2d and 4e crystallographic sites. In many of the $R_3T_4X_4$ compounds the magnetic ordering processes of the two R sites are independent [2–12].

[5] Author to whom any correspondence should be addressed.

We have previously carried out a study of the $Er_3Cu_4X_4$ compounds (X = Si, Ge and Sn) using high-resolution neutron powder diffraction, complemented by ^{166}Er and ^{119}Sn Mössbauer spectroscopy [7] and we observed quite distinct magnetic ordering processes at the Er 2d and 4e sites.

$R_3Ag_4Sn_4$ compounds with R = Sm and Gd were studied by Mazzone *et al* [13]. $Sm_3Ag_4Sn_4$ shows simple antiferromagnetic order whereas the antiferromagnetic order in $Gd_3Ag_4Sn_4$ is more complex, involving two transitions. It seems to be a general trend that the magnetic order in $R_3T_4X_4$ compounds becomes more complex with increasing R atomic number and, in an effort to study this behaviour, we have recently studied $Tb_3Ag_4Sn_4$ where we observed two distinct magnetic transitions at 28 K and 13 K [14]. In this paper we turn our attention to $Dy_3Ag_4Sn_4$. We have determined the magnetic ordering behaviour of the Dy sublattices by high-resolution neutron diffraction and we have also used ^{119}Sn Mössbauer spectroscopy to provide confirmation of the magnetic ordering modes determined by neutron diffraction.

2. Experimental methods

A stoichiometric quantity of the pure elements (Dy 99.9 wt%, Ag and Sn 99.999 wt%) was induction melted in sealed tantalum crucibles under high-purity argon. The alloyed buttons were then sealed under vacuum quartz tubes, annealed for 20 days at 873 K and then quenched in water. Cu Kα x-ray diffraction and electron microprobe analysis confirmed the majority phase to be the orthorhombic $Dy_3Ag_4Sn_4$ phase. Refinement of the neutron diffraction patterns showed the presence of less than 2 wt% of the ζ-phase $Ag_{79}Sn_{21}$.

Basic magnetic characterization was carried out on a Quantum Design PPMS system. ^{119}Sn transmission Mössbauer spectra were collected on a constant acceleration spectrometer using a 0.4 GBq ^{119m}Sn $CaSnO_3$ source with the sample in a helium flow cryostat. The spectrometer was calibrated using a ^{57}Co Rh source and an α-Fe foil. The spectra were fitted using a conventional non-linear least-squares minimization routine with line positions and intensities calculated from a full Hamiltonian solution.

Neutron diffraction measurements were made using the C2 multi-wire powder diffractometer on the NRU reactor at Chalk River Laboratories, Ontario. Temperatures down to 3.7 K were obtained using a closed-cycle refrigerator. The neutron wavelength used was 2.3719 Å. All refinements of the neutron and x-ray diffraction patterns were carried out using the FULLPROF/WinPlotr package [15, 16] and analysis of the neutron diffraction patterns included correction for the rather high neutron absorption by Dy.

3. Results and discussion

3.1. Crystal structure

The crystal structure of $Dy_3Ag_4Sn_4$ is orthorhombic with the space group *Immm* (#71). There are two Dy sites (2d and 4e), one Ag site (8n) and two Sn sites (4f and 4h), yielding two formula units per orthorhombic cell. The lattice parameters and atomic positions of $Dy_3Ag_4Sn_4$ were determined by high-resolution neutron powder diffraction at 300 K (figure 1). The lattice parameters are: $a = 15.1150(32)$ Å, $b = 7.2826(13)$ Å and $c = 4.5296(8)$ Å. The conventional refinement R-factors (%) for the 300 K pattern are: R(Bragg) = 10.5 and $R(F$-struct.) = 9.8. The refined atomic position parameters are given in table 1. The refined value of the overall isotropic thermal parameter B_{iso} at 300 K is 6.2(5) Å^2.

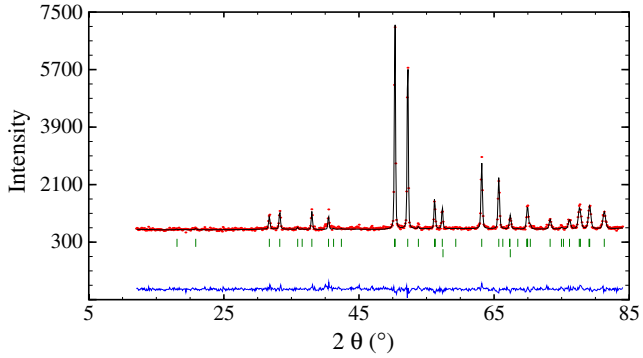

Figure 1. Neutron powder diffraction pattern of $Dy_3Ag_4Sn_4$ at 300 K. The upper set of Bragg markers is for $Dy_3Ag_4Sn_4$ while the lower set is for ζ-$Ag_{79}Sn_{21}$.

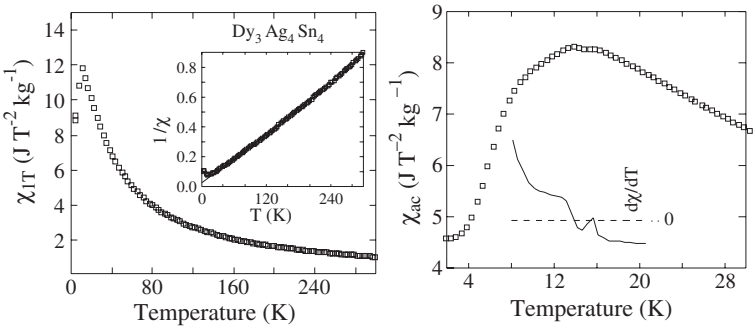

Figure 2. Left panel: DC susceptibility measured in a 1 T field (χ_{1T}) as a function of temperature for $Dy_3Ag_4Sn_4$. The inset shows a Curie–Weiss plot with fit described in the text. Right panel: $\chi_{ac}(T)$ in a drive field of 1 mT at 137 Hz below 30 K. Two very weak features at 13.8(3) and 15.8(3) K (more evident in the inset derivative shown as a solid line: $d\chi/dT$ versus T) may be associated with the transitions identified later from the neutron diffraction data.

Table 1. Atomic positions in $Dy_3Ag_4Sn_4$ at 300 K.

Atom	Site	x	y	z
Dy	2d	$\frac{1}{2}$	0	$\frac{1}{2}$
Dy	4e	0.1290(10)	0	0
Ag	8n	0.3286(19)	0.1981(35)	0
Sn	4f	0.2158(22)	$\frac{1}{2}$	0
Sn	4h	0	0.1952(53)	$\frac{1}{2}$

3.2. Magnetic susceptibility

The temperature dependence of the DC susceptibility measured in a field of 1 T shows evidence of a single magnetic transition near 15 K (left panel of figure 2). Fitting the high-temperature region of $\chi_{1T}(T)$ to a Curie–Weiss law (inset to left panel of figure 2) yields $\theta_{CW} = -5.6(7)$ K, confirming that the dominant exchange interactions are antiferromagnetic. The fit also yields an effective moment of 11.1(6) μ_B/Dy, fully consistent with the free-ion value of 10.65 μ_B/Dy. $\chi_{ac}(T)$, for $Dy_3Ag_4Sn_4$ in a drive field of 1 mT at 137 Hz (right panel of figure 2), shows a rounded maximum centred at ∼15 K, with weak features (amplitude less than 0.5%) at

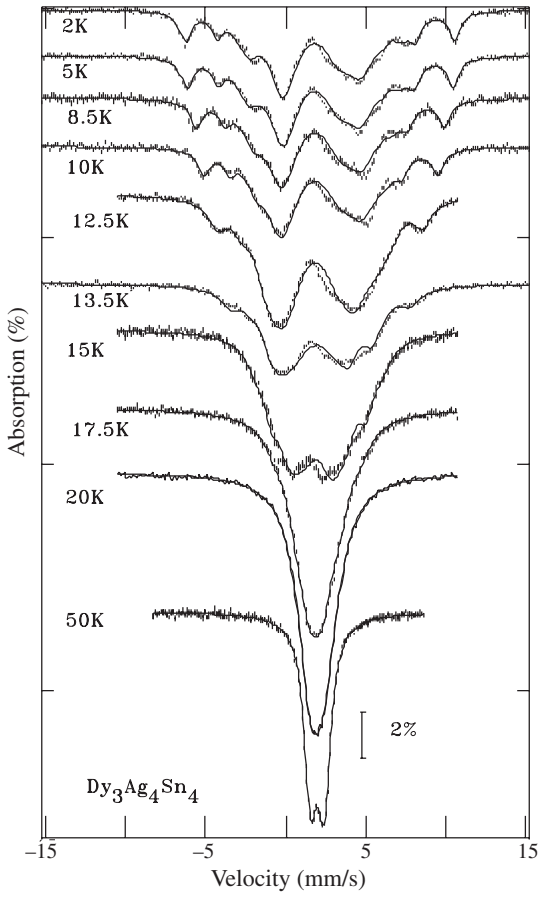

Figure 3. ^{119}Sn Mössbauer spectra of $Dy_3Ag_4Sn_4$ as a function of temperature. Solid lines are fits described in the text.

13.8(3) K and 15.8(3) K. These peaks are more evident in the derivative, and the zero-crossings of the derivative were used to determine the locations of the two features. Ordinarily, such minor deviations might be dismissed; however, as we will show below, they correspond closely with the behaviour observed in the Mössbauer and neutron diffraction data.

3.3. ^{119}*Sn Mössbauer spectroscopy*

The ^{119}Sn Mössbauer spectrum of $Dy_3Ag_4Sn_4$ at 2 K (figure 3) confirms that the material is magnetically ordered. The pattern is quite complex and cannot be fitted using the crystallographically required two equal area components corresponding to tin atoms in the 4f and 4h sites (see table 1). The central region of the spectrum is occupied by many overlapping and severely broadened lines, obscuring the spectral details; however, there is one quite sharp, well split, magnetic sextet in the pattern that does not suffer from overlap problems. This component was isolated and found to account for about one quarter of the total area. We therefore adopted a three-component fitting model with areas of 50%:25%:25% as the minimum deviation from the crystallographic constraints that would allow us to fit the spectra.

The three-site model provides an adequate description of the data over the temperature range shown in figure 3, with linewidths at 2 K of 0.81(1) mm s^{-1} and 0.91(2) mm s^{-1} being needed for the 7.38(7) T and 3.68(3) T components respectively. The sharp, 12.58(3) T

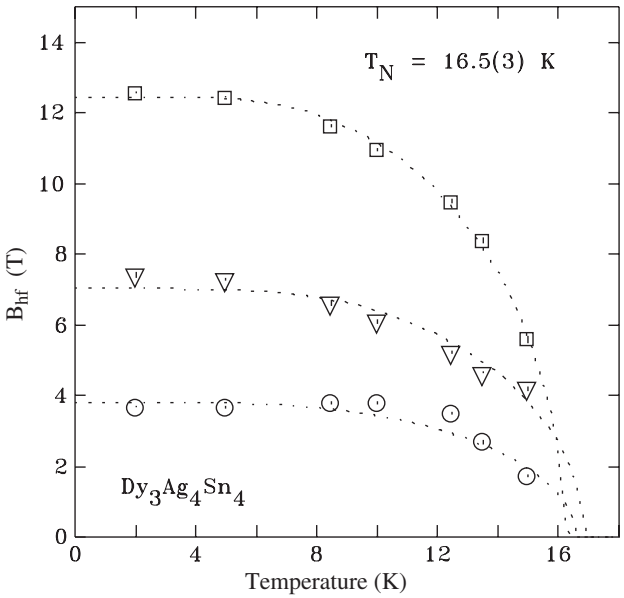

Figure 4. Temperature dependence of the hyperfine field (B_{hf}) for the three tin spectral components in $Dy_3Ag_4Sn_4$. Errors are shown within the plotted points and are less than 0.1 T in all cases. The dotted lines are fits to Brillouin functions used to estimate the ordering temperature.

component gave a linewidth of 0.40(2) mm s^{-1}, more typical of ^{119}Sn Mössbauer spectra. The deviations between the fits and the data likely reflect an incomplete modelling of the line broadening effects. By splitting one of the tin sites into two sub-components we are assuming that the magnetic ordering of the Dy moments is sufficiently complex as to create magnetically inequivalent Sn environments at one of the crystallographic sites. This complex ordering could also lead to slight variations in the magnetic environments even for nominally equivalent sites and thus cause some line broadening. We have modelled this additional broadening by simply increasing the width of all lines for a given component. It is clear that while this procedure misses some details in the patterns, it does provide a reasonable description of the global behaviour.

The temperature dependence of the hyperfine magnetic fields (B_{hf}) for the three tin components is shown in figure 4. The 12 T and 8 T components each account for 25% of the total spectral area, while the 4 T component makes up the balance. The fields for all three components appear to track together and yield a common transition temperature of 16.5(3) K. This corresponds to the upper of the two features noted in the χ_{ac} data in figure 2. While there may be some deviations from simple behaviour for the two smaller field sites above 12 K, we see no anomaly that could reliably be associated with the 14 K χ_{ac} feature. It is clear from figure 4 that by 14 K, B_{hf} is greatly reduced at all three sites and line overlap is a severe problem (figure 3). It is unlikely that any credible signature could be identified under such conditions.

3.4. Neutron diffraction

The neutron diffraction patterns in figure 5 clearly show the onset of magnetic ordering, with a large number of strong magnetic reflections developing on cooling through 16 K, consistent with our Mössbauer results. The lowest-temperature patterns are dominated by the purely magnetic $(0\ \frac{1}{2}\ 0)$ peak at $2\vartheta = 9.4°$. Closer examination reveals that the first magnetic peaks to appear on cooling are located at incommensurate positions and that while they initially dominate the patterns, they are gone by 10 K, and other magnetic reflections have replaced them.

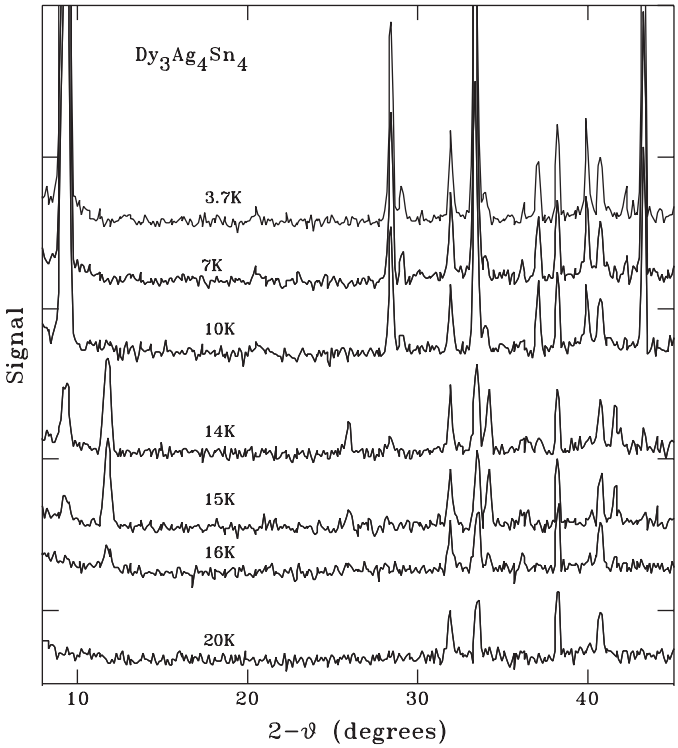

Figure 5. Neutron diffraction patterns for $Dy_3Ag_4Sn_4$, showing the onset of magnetic order at 16 K and the brief appearance of several incommensurate magnetic peaks around 14 K.

Figure 6 summarizes the temperature dependence of several of the stronger magnetic reflections seen in figure 5. Increasing the temperature from 3.7 K leads to the expected decrease in intensity for the magnetic peaks, and fitting this decrease to a Brillouin function yields an ordering temperature of 14.5(2) K. However, a set of incommensurate peaks appear as this temperature is approached and their intensities pass through a maximum as the original peaks disappear. All magnetic scattering is finally lost at 16.5(5) K. We note that the two characteristic temperatures derived from the neutron diffraction data correspond closely with those seen earlier in the $\chi_{ac}(T)$ data. Also, the final loss of magnetic scattering at 16.5(5) K is in perfect agreement with the ordering temperature derived from ^{119}Sn Mössbauer spectroscopy.

In figure 7 we show the neutron diffraction pattern of $Dy_3Ag_4Sn_4$ obtained at 3.7 K, at which temperature all Dy moments are ordered and the magnetic structure of $Dy_3Ag_4Sn_4$ is described by the propagation vector $\mathbf{k} = [0\ \frac{1}{2}\ 0]$, i.e. the magnetic structure is doubled along the *b*-axis. To investigate the possible ordering modes at the two Dy sites we carried out a representation analysis using the program SARA *h* [17]. Representation analysis for the Dy(2d) site with $\mathbf{k} = [0\ \frac{1}{2}\ 0]$ shows that the decomposition of the 2d-site magnetic representation comprises three one-dimensional representations (equation (1)):

$$\Gamma_{\mathrm{Mag}} = 1\Gamma_2^{(1)} + 1\Gamma_3^{(1)} + 1\Gamma_4^{(1)}. \tag{1}$$

The basis vectors of the 2d-site irreducible representations are given in table 2.

Representation analysis for the Dy(4e) site, with $\mathbf{k} = [0\ \frac{1}{2}\ 0]$, shows that the decomposition of the 4e-site magnetic representation comprises four one-dimensional representations

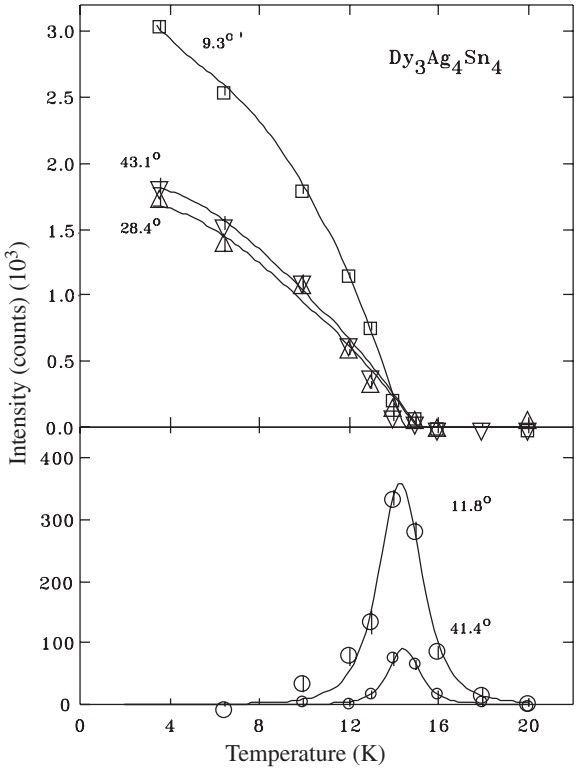

Figure 6. Temperature dependence of several strong magnetic reflections for $Dy_3Ag_4Sn_4$. The upper panel shows the peaks associated with the low-temperature commensurate ordering, while the lower panel shows those peaks associated with the incommensurate order that appears around 14 K.

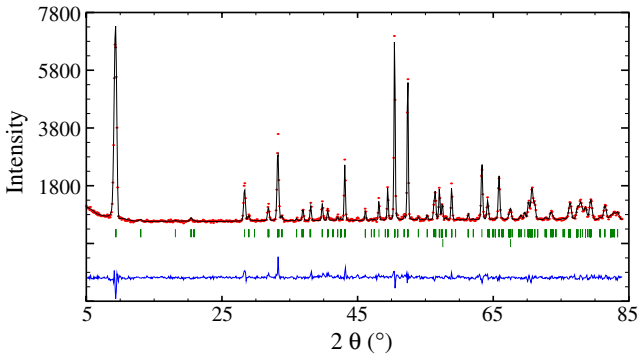

Figure 7. Neutron powder diffraction pattern of $Dy_3Ag_4Sn_4$ at 3.7 K.

Table 2. Representation analysis for the Dy(2d) site in $Dy_3Ag_4Sn_4$ with $\mathbf{k} = [0\ \frac{1}{2}\ 0]$. The atomic position of the primitive basis is $(\frac{1}{2}, 0, \frac{1}{2})$.

Representation	Basis vector	Atom 1
$\Gamma_2^{(1)}$	ψ_1	[0 1 0]
$\Gamma_3^{(1)}$	ψ_2	[1 0 0]
$\Gamma_4^{(1)}$	ψ_3	[0 0 1]

(equation (2)):

$$\Gamma_{\text{Mag}} = 1\Gamma_1^{(1)} + 2\Gamma_2^{(1)} + 2\Gamma_3^{(1)} + 1\Gamma_4^{(1)}. \tag{2}$$

The basis vectors of the 4e-site irreducible representations are given in table 3.

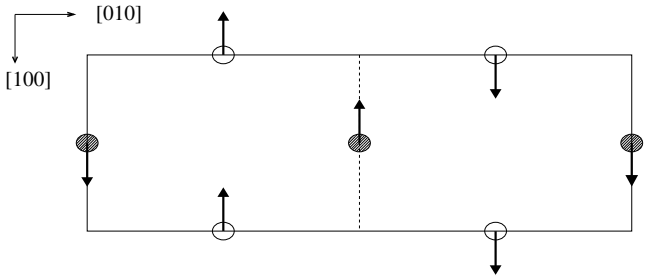

Figure 8. Magnetic structure of the Dy(2d) sublattice, projected onto the $z = 0$ plane. Only the Dy atoms are shown. The unshaded symbols correspond to $z = 0$ and the shaded symbols correspond to $z = \frac{1}{2}$.

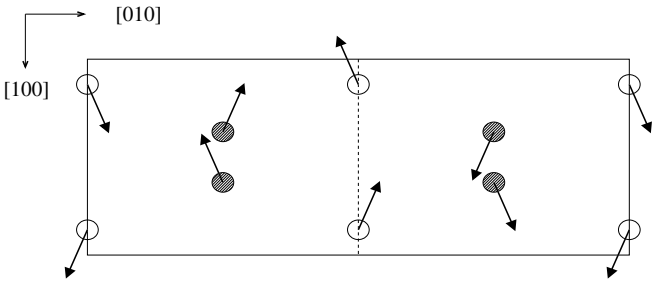

Figure 9. Magnetic structure of the Dy(4e) sublattice, projected onto the $z = 0$ plane. Only the Dy atoms are shown. The unshaded symbols correspond to $z = 0$ and the shaded symbols correspond to $z = \frac{1}{2}$.

Table 3. Representation analysis for the Dy(4e) site in $Dy_3Ag_4Sn_4$ with $\mathbf{k} = [0\ \frac{1}{2}\ 0]$. The atomic positions defining the non-primitive basis are $(x, 0, 0)$ and $(-x, 0, 0)$.

Representation	Basis vector	Atom 1	Atom 2
$\Gamma_1^{(1)}$	ψ_1	[0 0 1]	[0 0 $\bar{1}$]
$\Gamma_2^{(1)}$	ψ_2	[1 0 0]	[$\bar{1}$ 0 0]
$\Gamma_2^{(1)}$	ψ_3	[0 1 0]	[0 1 0]
$\Gamma_3^{(1)}$	ψ_4	[1 0 0]	[1 0 0]
$\Gamma_3^{(1)}$	ψ_5	[0 1 0]	[0 $\bar{1}$ 0]
$\Gamma_4^{(1)}$	ψ_6	[0 0 1]	[0 0 1]

We obtained the best fit to the 3.7 K neutron diffraction pattern of $Dy_3Ag_4Sn_4$ with the Dy moments ordering under the $\Gamma_3^{(1)}$ irreducible representation. The Dy(2d) moments order with the basis vector ψ_2, aligned along the [100] direction (a-axis). The refined Dy(2d) magnetic moment in $Dy_3Ag_4Sn_4$ at 3.7 K is 8.3(3) μ_B. In figure 8 we show the magnetic structure of the Dy(2d) sublattice.

The Dy(4e) moments order with the basis vectors ψ_4 and ψ_5, aligned within the (001) plane (ab-plane). The refined Dy(4e) magnetic moment at 3.7 K is [7.6(2), 1.4(4), 0] μ_B, yielding a net Dy(4e) moment of 7.7(5) μ_B. In figure 9 we show the magnetic structure of the Dy(4e) sublattice.

The neutron diffraction pattern obtained at 14 K (figure 10) indicates that one of the Dy sublattices is incommensurate. We obtained the best fit to the pattern with the Dy(2d) site

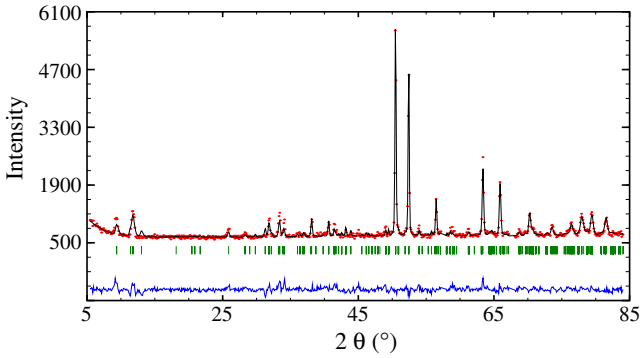

Figure 10. Neutron powder diffraction pattern of $Dy_3Ag_4Sn_4$ at 14 K.

ordered as at 3.7 K, i.e. with a propagation vector $\mathbf{k} = [0\ \frac{1}{2}\ 0]$ and a moment of 4.8(5) μ_B along [100]. The Dy(4e) site orders incommensurately with $\mathbf{k} = [0\ 0.628(1)\ 0]$ and a moment of [4.0(5) 1.3(8) 0] μ_B, leading to a net Dy(4e) moment of 4.2(9) μ_B.

The evolution of magnetic order at the Dy(4e) site from incommensurate near the onset of order at 16.5(5) K, to commensurate on further cooling, is common to many rare-earth intermetallic compounds [19]. Mean-field modelling that includes the Fourier components of the exchange field associated with complex magnetic structures [20] has shown that while long-period commensurate or incommensurate structures may be stable just below T_N, they are generally unstable at 0 K and therefore must exhibit a transition to a shorter period commensurate structure on cooling. The incommensurate → commensurate transition is expected to be a discontinuous step in period as the magnetic structure locks to the lattice [20]. Both the ordering sequence and the predicted lock-in are observed here at the Dy(4e) site.

3.5. ^{119}Sn Mössbauer spectroscopy

There are two, equipopulous Sn sites in the $Dy_3Ag_4Sn_4$ structure but, as mentioned earlier, two magnetic sextets are insufficient to fit the observed spectra; we found that three sextets in the area ratio 50%:25%:25% are required. Sn is non-magnetic and the hyperfine magnetic field observed at the ^{119}Sn nucleus is due to surrounding magnetic moments, i.e. a transferred hyperfine field. We have determined the nearest-neighbour environments of the two Sn sites in $Dy_3Ag_4Sn_4$ by finding their Wigner–Seitz cells using the BLOKJE program [18].

The Sn(4f) Wigner–Seitz cell has 11 faces and a volume of 20.6 Å^3, encompassing 6 Ag and 5 Dy neighbours. The Dy neighbours comprise one Dy(2d) site at a distance of 3.26 Å, two Dy(4e) sites at 3.26 Å and a further two Dy(4e) sites at 3.87 Å. The Sn(4h) Wigner–Seitz cell has 9 faces and a volume of 21.2 Å^3, encompassing 6 Dy, 2 Ag and 1 Sn neighbours. The Dy neighbours comprise two Dy(2d) sites at a distance of 3.17 Å and four Dy(4e) sites at 3.31 Å.

The magnetic structures of the Dy sublattices in $Dy_3Ag_4Sn_4$, determined from our neutron diffraction data and shown in figures 8 and 9, indicate that all four Sn(4f) sites have the same relative arrangement of their five magnetic Dy neighbours and hence should experience the same transferred hyperfine magnetic field. In contrast, the four Sn(4h) sites split into two subgroups, having different relative arrangements of their magnetic Dy neighbours. Consequently, these sub-groups may be expected to experience different transferred hyperfine fields. Atoms $(0\ y\ \frac{1}{2})$ and $(\frac{1}{2}\ \frac{1}{2}\ -y\ 0)$ form one sub-site while atoms $(0\ \overline{y}\ \frac{1}{2})$ and $(\frac{1}{2}\ \frac{1}{2}\ +y\ 0)$ form the other. Thus, the observed 50%:25%:25% makeup of the ^{119}Sn Mössbauer spectra is fully consistent with the magnetic structure of the Dy sublattices in $Dy_3Ag_4Sn_4$ we deduced from our neutron diffraction data.

4. Conclusion

We have determined the magnetic ordering behaviour of $Dy_3Ag_4Sn_4$ by high-resolution neutron diffraction, complemented by ^{119}Sn Mössbauer spectroscopy. $Dy_3Ag_4Sn_4$ orders at 16(1) K in a complex antiferromagnetic structure in which the Dy moments at the 2d sites are aligned commensurately along [100] with a doubled magnetic cell along [010], i.e. a propagation vector $\mathbf{k} = [0\ \frac{1}{2}\ 0]$. The Dy moments at the 4e sites are aligned incommensurately in the (001) plane with a propagation vector $\mathbf{k} = [0\ 0.628(1)\ 0]$. At 14(1) K Dy(4e) 'locks-in' to the same doubled cell as the Dy(2d) site. The transferred hyperfine fields at the Sn sites clearly demonstrate this magnetic structure.

Acknowledgments

We are grateful to Lachlan Cranswick, Chalk River Laboratories, for assistance during the neutron diffraction experiments. This work was supported in part by grants from the Natural Sciences and Engineering Research Council of Canada and Fonds pour la formation de chercheurs et l'aide à la recherche, Québec. FC wishes to thank the MIUR for the for research support: PRIN2004 'Caratterizzazione Chimico fisica di composti intermetallici in forma di bulk e in forma di film'. JMC is grateful to the Australian Research Council and The University of New South Wales (FRGP scheme) for financial support. JMC also wishes to thank the Centre for the Physics of Materials, Department of Physics, McGill University, for its hospitality during a sabbatical visit when much of this work was carried out.

References

[1] Rieger W 1970 *Monat. Chem.* **101** 449–62
[2] Szytula A, Wawrzyńska E, Penc B, Stüsser N and Zygmunt A 2003 *Physica* B **327** 167–70
[3] Wawrzyńska E, Hernández-Velasco J, Penc B, Szytula A and Zygmunt A 2003 *J. Magn. Magn. Mater.* **264** 192–201
[4] Wawrzyńska E, Hernández-Velasco J, Penc B, Sikora W, Szytula A and Zygmunt A 2003 *J. Phys.: Condens. Matter* **15** 5279–96
[5] Wawrzyńska E, Penc B, Hernández-Velasco J, Szytula A and Zygmunt A 2003 *J. Alloys Compounds* **350** 68–71
[6] Wawrzyńska E, Penc B, Stüsser N, Szytula A and Tomkowicz Z 2003 *Solid State Commun.* **126** 527–30
[7] Ryan D H, Cadogan J M, Gagnon R and Swaison I P 2004 *J. Phys.: Condens. Matter* **16** 3183–98
[8] Wawrzyńska E, Hernández-Velasco J, Penc B, Szytula A and Tomala K 2004 *J. Phys.: Condens. Matter* **16** 7535–44
[9] Wawrzyńska E, Hernández-Velasco J, Penc B and Szytula A 2004 *J. Phys.: Condens. Matter* **16** 45–52
[10] Szytula A, Wawrzyńska E, Penc B, Stüsser N, Tomkowicz Z and Zygmunt A 2004 *J. Alloys Compounds* **367** 224–9
[11] Wawrzyńska E, Hernández-Velasco J, Penc B, Rams N and Szytula A 2005 *J. Magn. Magn. Mater.* **288** 111–20
[12] Wawrzyńska E, Hernández-Velasco J, Penc B and Szytula A 2004 *J. Magn. Magn. Mater.* **280** 234–42
[13] Mazzone D, Riani P, Napoletano M and Canepa F 2005 *J. Alloys Compounds* **387** 15–9
[14] Perry Laura K, Ryan D H, Canepa F, Napoletano M, Mazzone D, Riani P and Cadogan J M 2006 *J. Appl. Phys.* **99** 08J502(3)
[15] Rodríguez-Carvajal J 1993 *Physica* B **192** 55–69
[16] Roisnel T and Rodríguez-Carvajal J 2001 *Mater. Sci. Forum* **378–381** 118–23
[17] Wills A S 2000 *Physica* B **276–8** 680 (program available from ftp://ftp.ill.fr/pub/dif/sarah/)
[18] Gelato L 1981 *J. Appl. Crystallogr.* **14** 151–3
[19] Szytula A and Leciejewicz J 1994 *Handbook of Crystal Structures and Magnetic Properties of Rare-Earth Intermetallics* (Boca Raton, FL: CRC Press)
[20] Gignoux D and Schmitt D 1993 *Phys. Rev.* B **48** 12682–91